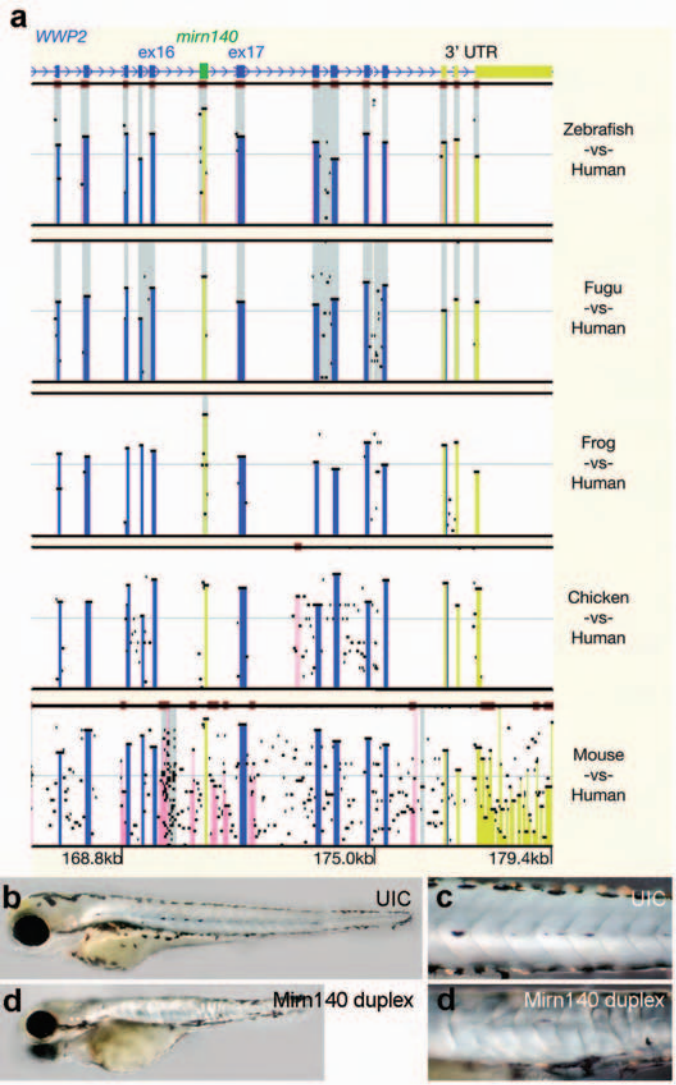


Supplementary Figure 1. Vertebrate genomes have mirn140 in the orthologous intron of the orthologous gene and Mirn140 overexpression causes somite and body axis defects. (a) Human *mirn140* lies in the intron between exon 16 and 17 of *WWP2* (OTTHUMG00000073640, NM_ 199423), which encodes a WW domain containing E3 ubiquitin protein ligase 2. Genomic sequences of the *WWP2* orthologs from various vertebrates were aligned by Zpicture plots (http://zpicture.dcode.org) to display regions of sequence similarity. Percent nucleotide identity over a 100 bp sliding window is plotted on the vertical axis comparing the indicated species with regard to a 13 kb portion of the human *WWP2* gene Along the top herringbone line, blue rectangles show the positions of exons in the human gene; the green rectangle shows the position of the human *mirn140*; and the yellow rectangles show the 3' untranslated region (UTR). The plots show that *mirn140* and exon structure are conserved in the *WWP2* ortholog of zebrafish (*Danio rerio*, ENSDARG00000061345), fugu pufferfish (*Takifugu rubripes*, SINFRUT00000158314), frog (*Xenopus tropicalis*, ENSXETG00000017879), chicken (*Gallus gallus*, ENSGALG00000000699), and mouse (*Mus musculus*, ENSMUSG00000031930), which has substantial additional conservation of non-coding genomic regions with human. (b-e) At 72 hpf, compared to uninjected controls (b,c), fish injected with Mirn140 duplex showed shortened body length (d) and disrupted somites (e), phenotypes that are also present in mouse *Pdgfra* mutants.

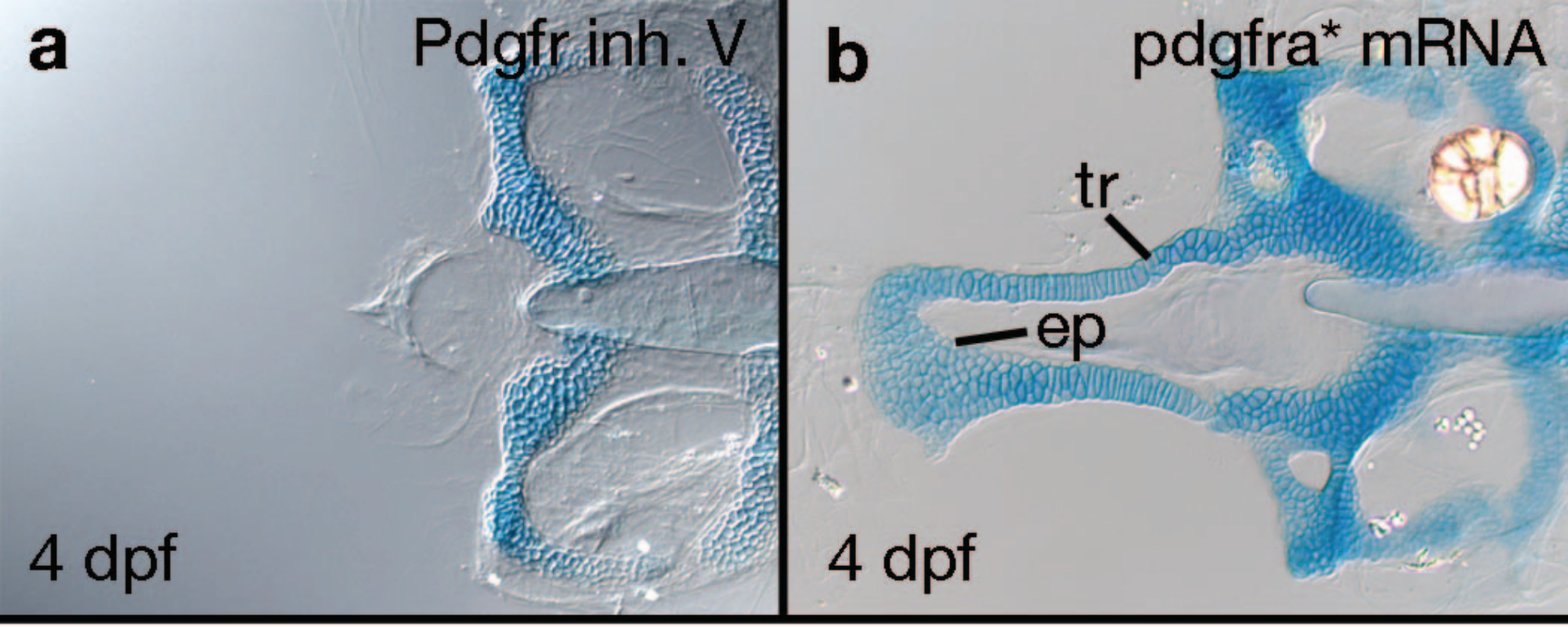


Supplementary Figure 2. *b1059* is a mutant allele of *pdgfra*. (a) Inhibition of Pdgf receptor signaling phenocopies the cleft palate phenotype of *b1059* mutants. (b) Injection of *pdgfra* mRNA into *b1059* mutants rescues the palatal skeleton.

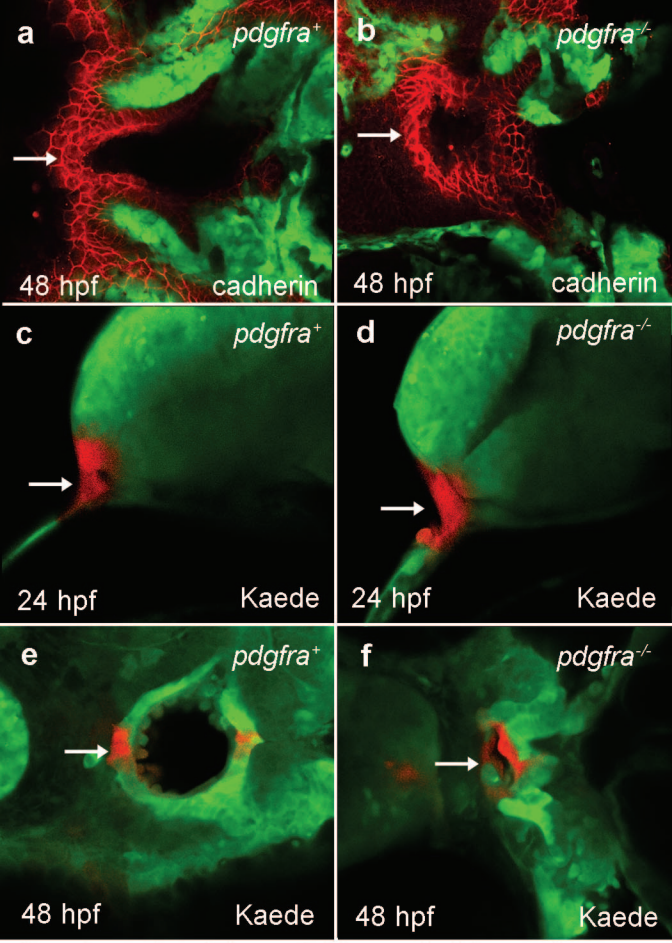


Supplementary Figure 3. The roof of the oral ectoderm is present in *pdgfra* mutants. (a,b) Anti-pan-cadherin antibody in *fli1:EGFP* transgenic embryos staining demonstrates an epithelium is present at the roof of the mouth in *pdgfra*$^{+}$ (a) and *pdgfra*$^{-/-}$ embryos (b). (c-f) Kaede photoconversion demonstrates that the 24 hpf fate map of the upper lip is not altered in *pdgfra*$^{-/-}$ embryos. Photoconversion of the anterior-most ectoderm at 24 hpf (c,d) labels the upper (arrow) and lower lips at 48 hpf (e,f) in *pdgfra*$^{+}$ (c,e) and *pdgfra*$^{-/-}$ (d,f) embryos.

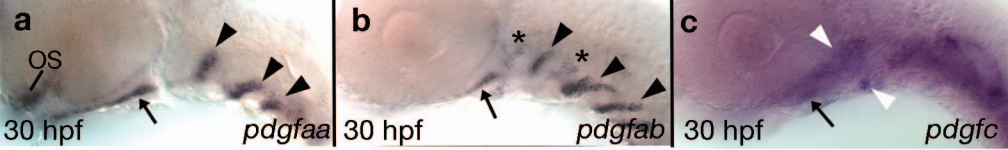


Supplementary Figure 4. Facial epithelia express ligands for Pdgfra as crest cells are condensing in the pharyngeal arches. (a-c) Lateral views of 30 hpf wild-type embryos stained with riboprobe to *pdgfaa* (a), *pdgfab* (b), or *pdgfc* (c). All ligands are expressed in the oral ectoderm (arrows), although the expression of *pdgfab* appears restricted to the oral ectoderm posterior to the eye. Expression of *pdgfaa* also labels the optic stalk (os). Transcripts for both *pdgfaa* and *pdgfab* are detected in the pharyngeal endoderm (a,b black arrowheads) and *pdgfab* is expressed in the arch mesodermal core (b, asterisks). The surface ectoderm overlying the first pharyngeal arch expresses *pdgfc* (c, white arrowhead).

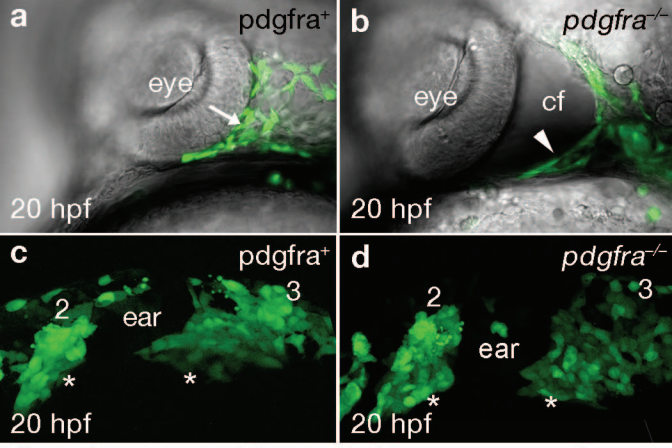


Supplementary Figure 5. Many crest cells reach their targets in *pdgfra* mutants. (a,b) Merged confocal fluorescent and DIC images of migratory neural crest cells in *pdgfra*$^{+}$ (a) and *pdgfra*$^{-/-}$ (b) embryos. (a) Crest cells migrating behind the eye to reach the oral ectoderm normally fill the region immediately posterior to the eye (arrow). (b) In *pdgfra* mutants, however, neural crest cells do not enter this cell-free region posterior to the eye (cf), although a small subset of neural crest reach the oral ectoderm by a circuitous route (arrowhead). (c,d) Lateral views of the second and third neural crest streams in *sox10:EGFP* transgenic *pdgfra*$^{+}$ (c) and *pdgfra*$^{-/-}$ (d) embryos. The migration of second and third neural crest streams, anterior and posterior of the ear, respectively, into the pharyngeal arches is normal in *pdgfra* mutants.
The asterisks indicate the ventral limit of each pharyngeal arch.

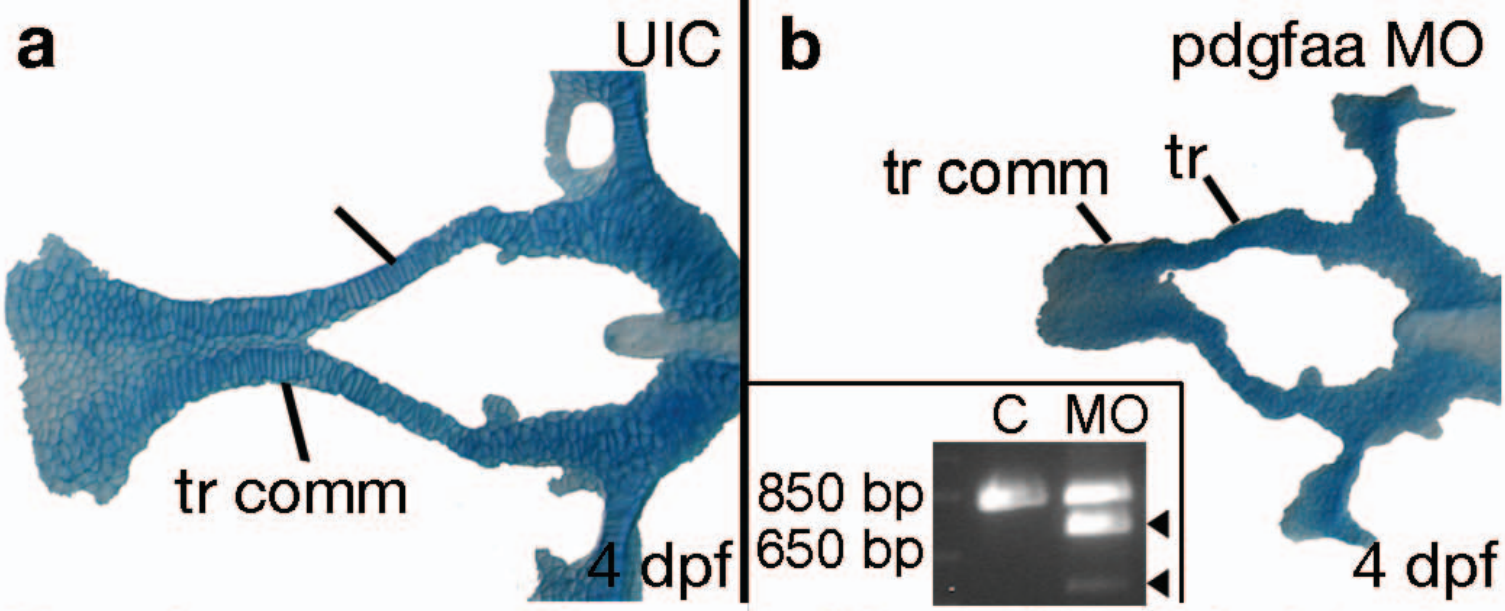


Supplementary Figure 6. The ethmoid plate is lost in *pdgfaa* morpholino injected embryos. Flat mounted 4 dpf palatal skeleton from control (a) and *pdgfaa* morpholino-injected (b) embryos. In *pdgfaa* morpholino injected embryos, the trabeculae (tr) extend to the midline, forming the trabecular communis (tr comm), but the ethmoid plate (ep) is lost. In 8% of embryos (n=37) the palatal skeleton was clefted (data not shown), similar to *pdgfra* mutants. (b, inset) Injection of *pdgfaa* morpholino disrupts splicing of *pdgfaa* RNA. The morpholino targets the intron 2/exon 3 boundary and the approximately 750 bp major splice variant observed is the size predicted following loss of exon three.

Supplementary table 1. Predicted Mirn140 (miR-140) binding sites in the 3′ UTR of various vertebrate *pdgfra* orthologs

| Species | *mirn140(miR-140)* | Mature Mirn140 sequence | *pdgfra* gene | 1st Predicted Target Site | 2nd Predicted Target site |
|---|---|---|---|---|---|
| *Danio rerio* zebrafish | *dre-miR-140* ① | 5′CAGUGGUUUUACCCUAUGGUAG3′ | ENSDART00000011915 ② | GAUGGUAUCCCAUUUUGGUGAC<br>:\|:\|\|\| \| \|\|\|\|\|\|\|\|<br>GAGCUAUAAAG-AAAACCACUA<br>422-442③ | |
| *Takifugu rubripes* pufferfish | *fru-miR-140* | 5′CAGUGGUUUUACCCUAUGGUAG3′ | SINFRUT00000170924 | GAUGGUAUCCCA------UUUUGGUGAC<br>\| :\|\|\|\| \|\|\| \|\|\|\|\|\|\|<br>CAAUCAUACGGUACAUAGUUAACCACUA<br>343-370 | GAUGGUAUCCCAUUUUGGUGAC<br>\|\|:\|\| \| : :\|\|\|\|\|\|<br>CUGCCUCC-AGCUGUGCCACUG<br>1057-1077 |
| *Xenopus tropicalis* Frog | *xtr-miR-140* | 5′AGUGGUUUUACCCUAUGGUAG3′ | ENSXETG00000021035 | GAUGGUAUCCCA-UUUUGGUGAc<br>:\|\|\|: \|\| \| \|\|\|\|\|\|\|\|\|<br>UUACUCAAGCAUCAAAACCACUU<br>464-486 | GAUGGUAUCCCAUUUUGGUGAc<br>\|\|\|::: \|\|\|\| :\|\|\|:\|\|<br>CUAUUGCAGGGAUUUGCCAUUG<br>1195-1216 |
| *Gallus gallus* Chicken | *gga-miR-140* | 5′AGUGGUUUUACCCUAUGGUAG3′ | ENSGALT00000009189 | GAUGGUAUCCCAUUUUGGUGAc<br>: : \| \|\|\|\|\|\|\|\|\|<br>UGCUACACAGAGAAAACCACUU<br>57-78 | GAUGGUAUCCCA-UUUUGGUGAc<br>: \| \| \| \|\|\|\|\|\|\|\|\|<br>UGAAGAACAUGCAAAAACCACUC<br>502-524 |
| *Mus musculus* Mouse | *mmu-miR-140* | 5′CAGUGGUUUUACCCUAUGGUAG3′ | ENSMUST00000000476 | GAUGGUAUCCCAUUUUGGUGAC<br>\|\|\|\|\|\|\|\|\|<br>GAUAACCUUAAGAAAACCACUU<br>43-64 | GAUGGUAUCCCAUUUUGGUGAC<br>: \| \| \|\|\|\|\|\|\|\|\|<br>UGAAGUACAUGCAAAACCACUU<br>488-509 |
| *Rattus norvegicus* Rat | *rno-miR-140* | 5′AGUGGUUUUACCCUAUGGUAG3′ | ENSRNOT00000003077 | GAUGGUAUCCCAUUUUGGUGAc<br>\|\| \|\|\|\|\|\|\|\|\|<br>GAUCCCCUUAAGAAAACCACUU<br>47-68 | GAUGGUAUCCCAUUUUGGUGAc<br>: \| \| \|\|\|\|\|\|\|\|\|<br>UGAAGUACAUGCAAAACCACUU<br>480-501 |
| *Canis familiaris* Dog | ENSCAFG00000020455 | 5′CAGUGGUUUUACCCUAUGGUAG3′ | ENSCAFT00000003270 | GAUGGUAUCCCAUUUUGGUGAC<br>\|\| \| \|\|\|\|\|\|\|\|\|<br>GAUCCCUUUAAGAAAACCACUU<br>50-71 | GAUGGUAUCCCAUUUUGGUGAC<br>: \| \| \|\|\|\|\|\|\|\|\|<br>UGAAGUACAUGCAAAACCACUU<br>492-513 |
| *Pan troglodytes* chimpanzee | *ptr-miR-140* | 5′AGUGGUUUUACCCUAUGGUAG3′ | ENSPTRT00000029945 | GAUGGUAUCCCAUUUUGGUGAc<br>\|\| \|\|\|\|\|\|\|\|\|<br>GAUCCCGUUCAGAAAACCACUU<br>45-66 | GAUGGUAUCCCAUUUUGGUGAc<br>\| \| \|\|\|\|\|\|:\|<br>AGAAGUGCAUGAAAAACCAUUU<br>486-507 |
| *Homo sapiens* Human | *hsa-miR-140* | 5′AGUGGUUUUACCCUAUGGUAG3′ | ENST00000381354 | GAUGGUAUCCCAUUUUGGUGAc<br>\|\| \|\|\|\|\|\|\|\|\|<br>GAUCCCGUUCAGAAAACCACUU<br>44-66 | GAUGGUAUCCCAUUUUGGUGAc<br>\| \| \|\|\|\|\|\|:\|<br>AGAAGUGCAUGAAAAACCAUUU<br>487-508 |

① Green indicates mirn140. ② Yellow indicates *pdgfra*, with predicted Mirn140 binding sites in the 3′UTR (5′ to left, 3′ to right). Prediction programs: MicroInspector (http://mirna.imbb.forth.gr/microinspector)[1] and miRBase (http://microrna.sanger.ac.uk/targets/v4)[2]. ③ Position of first and last nucleotides of the predicted *miR-140* binding site in 3′UTR of *pdgfra* gene counted from after the stop codon.


1. Rusinov, V., Baev, V., Minkov, I.N. & Tabler, M. MicroInspector: a web tool for detection of miRNA binding sites in an RNA sequence. *Nucleic Acids Res* **33**, W696-700 (2005).
2. Griffiths-Jones, S. miRBase: the microRNA sequence database. *Methods Mol Biol* **342**, 129-38 (2006).

Supplementary table 2. Oligo sequences.

| | Oligo name | Sequence |
|---|---|---|
| PCR primers | dCAP-F | 5'-TGTCTCCAAAGGAAGCGTG-3' |
| | dCAP-R | 5'-ACCGAGAGAGAAGATCTCCCATAACTAG-3' |
| | pdgfraUTR-F | 5'-TCTGCGTCATCTTGTCACTTTTTCTTCAC-3' |
| | pdgfraUTR-R | 5'-AACACAGCCATTTTCTTCATTTTAGGAC-3' |
| | nog3UTR-F | 5'-GAAATAAGCTCCGCACTCATCCTCACAT-3' |
| | nog3UTR-R | 5'-TCCATTCCCCTTATATTTACAGCACACCA-3' |
| | pdgfraF-F | 5'-TCATGTTCCCGGTGCTGCC-3' |
| | pdgfraF-R | 5'-GGGCTCCATAAGACTGAGGTGAAG-3' |
| | pdgfaaP-F | 5'-TGGGACACTTTTGGACCACAGG-3' |
| | pdgfaaP-R | 5'-TCGTTTTTCAGGCTGTCGTTG-3' |
| | pdgfabP-F | 5'-TGACATTGGAAGGAGATGAGAACC-3' |
| | pdgfabP-R | 5'-TTATTGAATATCCTTGTTGATCAGTGC-3' |
| | pdgfcP-F | 5'-CCAAATGATTCCGTTGCTTCTG-3' |
| | pdgfcP-R | 5'-GCGTCTTCTCTCTGGGACTGATT-3' |
| | primirn140-F | 5'-GCAAGTCAAACCCTGTAGCATCCCGTT-3' |
| | primirn140-R | 5'-GCGAGCCGATAGAGCGATTGTTT-3' |
| MO oligos | *mirn140* MO (mature) | 5'-CTACCATAGGGTAAAACCACTG-3'; |
| | *mirn140* MO (Dicer inhibitor) | 5'-GACGTAACCTACCATAGGGTAAAACCACTGA-3' |
| | *pdgfaa* I1E2 | 5' GGAATTGGTGCTTCCTGTTAAAGA 3' |
| | *pdgfaa* I2E3 | 5' CCTCCAGCACTTCATTCTCTGCAAC |
| | *p53* MO | 5'-GCGCCATTGCTTTGCAAGAATTG-3' |
| RNA oligos | Mirn140 | 5'-CAGUGGUUUUACCCUAUGGUAG-3' |
| | Mirn140 mismatch | 5'-CACACCAAGAACCCUAUGGUAG-3' |
| | Mirn140* | 5'-UACCACAGGGUAGAACCACGGAC-3' |
| LNA oligo | *mirn140-LNA* | 5'-CtACcATaGGgTAaAAcCAcTG-3'<br>(lowercase nucleotides represent LNA nts) |